

58 **Abstract**

59

60 *Objective*

61 Functional networks derived from resting-state scalp EEG from people with idiopathic (genetic)
62 generalized epilepsy (IGE) have been shown to have an inherent higher propensity to generate
63 seizures than those from healthy controls when assessed using the concept of brain network
64 ictogenicity (BNI). Herein we test whether the BNI framework is applicable to resting-state MEG and
65 whether it may achieve higher classification accuracy relative to previous studies using EEG.

66

67 *Methods*

68 The BNI framework consists in deriving a functional network from apparently normal brain activity,
69 placing a mathematical model of ictogenicity into the network and then computing how often such
70 network generates seizures in silico. We consider data from 26 people with juvenile myoclonic
71 epilepsy (JME) and 26 healthy controls.

72

73 *Results*

74 We find that resting-state MEG functional networks from people with JME are characterized by a
75 higher propensity to generate seizures (i.e. BNI) than those from healthy controls. We found a
76 classification accuracy of 73%.

77

78 *Conclusions*

79 The BNI framework is applicable to MEG and capable of differentiating people with epilepsy from
80 healthy controls. The observed classification accuracy is similar to previously achieved in scalp EEG.

81

82 *Significance*

83 The BNI framework may be applied to resting-state MEG to aid in epilepsy diagnosis.

84

85

86

87 **Highlights**

- 88 • Computational modelling is combined with MEG to differentiate people with juvenile
89 myoclonic epilepsy from healthy controls.
- 90 • Brain network ictogenicity (BNI) was found higher in people with juvenile myoclonic epilepsy
91 relative to healthy controls.
- 92 • BNI's classification accuracy was 73%, similar to previously observed using scalp EEG.

93

94

95

96 **Keywords**

97 epilepsy diagnosis; juvenile myoclonic epilepsy; biomarker; MEG; functional connectivity;
98 phenomenological model;

99

100

101

102

103

104

105

106

107

108

109

110

111

112

113

114

115

116

1. Introduction

117

118 Epilepsy is one of the most common neurological disorders with an estimated 5 million new diagnosis
119 each year (WHO, 2019). The diagnosis of epilepsy is based on clinical history and supported by
120 clinical electroencephalography (EEG). The presence of interictal spikes in the routine scalp EEG
121 recordings is one of the most valuable biomarkers of epilepsy (Pillai and Sperling, 2006). However,
122 the presence of interictal epileptiform discharges (IED) in a routine EEG is low, ranging between 25
123 and 56% (Smith, 2005; Benbadis et al., 2020). Furthermore, about 10% of people with epilepsy do not
124 show IEDs even after repeated or prolonged EEG (Smith, 2005; Benbadis et al., 2020). On the other
125 hand, specificity is also suboptimal, ranging between 78 and 98% (Smith, 2005), which, for example,
126 may delay the diagnosis of psychogenic nonepileptic attacks by 7 to 10 years (Benbadis, 2009).

127
128 The low sensitivity of IEDs results from IEDs being typically rare events. This may be a consequence
129 of their sources being deep in the brain and/or the extent of cortex involved in epileptic activity being
130 undetectable at the scalp surface (Pillai and Sperling, 2006). Consequently, much of the routine
131 clinical EEG recording consists of brain activity that appears normal to visual inspection, which
132 without other visible disturbances in background rhythms is considered non-informative. However,
133 growing evidence suggests that such sections of interictal EEG without IEDs may be used to inform
134 epilepsy diagnosis (e.g. Larsson and Kostov, 2005; Schmidt et al., 2016; Verhoeven et al., 2008).
135 Larsson and Kostov (2005) showed that there is a shift in the peak of the alpha power towards lower
136 frequencies in interictal EEG from people with both focal and generalized epilepsy. More recently,
137 Abela et al. (2019) found that a slower alpha rhythm may be an indicator of seizure liability. Other
138 studies have used graph theory to test whether functional networks derived from interictal EEG differ
139 from EEG obtained from healthy controls. It has been found that functional networks from people with
140 epilepsy are more “regular” (i.e. higher path lengths between nodes) and deviate more from small-
141 world structures than those found in healthy controls (Horstmann et al., 2010; Quraan et al., 2013).
142 Functional network alterations inferred from resting-state EEG have also been used to differentiate
143 children with focal epilepsy from healthy children (van Diessen et al., 2013, 2016). Furthermore,
144 resting-state EEG functional networks from people with IGE were shown to have more functional
145 connections than healthy controls (Chowdhury et al., 2014). Functional networks inferred from
146 interictal EEG from people with temporal lobe epilepsy have also been shown to differ from those
147 from healthy controls (Coito et al., 2016).

148
149 All these studies show that functional networks based on apparently normal EEG may aid in the
150 diagnosis of epilepsy. However, these studies lack mechanistic insights as to why such differences
151 may be related to epilepsy. To build such understanding, we and others have proposed to use
152 mathematical models of epilepsy to assess the functional networks and elucidate as to why a brain
153 may be prone to generate seizures (Schmidt et al., 2014, 2016; Petkov et al., 2014; Lopes et al.,
154 2019). In particular, we showed that resting-state EEG functional networks from people with IGE are
155 more prone to support synchronization phenomena and the emergence of seizure-like activity than
156 those from controls (Schmidt et al., 2014; Petkov et al., 2014). To quantify the differences, we
157 introduced the concept of brain network ictogenicity (BNI), i.e. a measure of how likely a functional
158 network is of generating seizures *in silico* (Petkov et al., 2014).

159
160 For the BNI to be useful for diagnosing people with epilepsy from apparently normal brain activity, we
161 relied on the assumption that the ability of a brain to generate seizures is an enduring feature that
162 should be identifiable during interictal periods. We further assumed that such underlying closeness to
163 seizures is captured by the properties of functional networks. We then assess the capacity of a given
164 functional network to generate seizures by estimating BNI through computer simulations that produce
165 long-term activity from which the volume of epileptiform activity can be evaluated. People with
166 epilepsy were therefore assumed to have resting-state functional networks that were more ictogenic,
167 i.e. that had a higher propensity to generate seizures as estimated by the BNI, compared to healthy
168 people. Using this framework on a dataset comprising 30 people with IGE and 38 healthy controls it
169 was found 100% specificity at 56.7% sensitivity, and 100% sensitivity at 65.8% specificity (Schmidt et
170 al., 2016).

171
172 In the current study, we aim to test whether the BNI concept may be equally useful when applied to
173 resting-state MEG data (i.e. its generalizability to a different data modality), and whether it may yield
174 superior diagnostic power of epilepsy relative to previous applications of BNI to resting-state EEG
175 data. In particular, we aim to find whether BNI may be capable of differentiating juvenile myoclonic
176 epilepsy (JME) from healthy controls, using MEG data, and observe how classification accuracy
177 compares to previous studies of BNI on scalp EEG (Schmidt et al., 2014, 2016). Since MEG has the

178 advantage, relative to EEG, of neuromagnetic fields being minimally perturbed by brain tissue, skull
179 and scalp (Supek and Aine, 2016), one may expect that MEG-derived functional networks may be
180 more reliable than those from EEG, which in turn may enhance the BNI's ability to differentiate people
181 with generalized epilepsy from healthy controls.

182
183

184 **2. Methods**

185
186

186 **2.1. Participants**

187
188

188 We used resting-state MEG data obtained from 26 people with JME and 26 healthy controls. The
189 individuals with epilepsy were recruited from a specialist clinic for epilepsy at University Hospital of
190 Wales in Cardiff, and the healthy individuals were volunteers who had no history of significant
191 neurological or psychiatric disorders. The healthy group was age and gender matched to the epilepsy
192 group. The age range in the epilepsy group was 17 to 47, median 27 years, and in the control group
193 was 18 to 48, median 27 years. There were 7 males in the epilepsy group and 7 males in the control
194 group. Individuals in the epilepsy group had a number of different seizure types and were taking anti-
195 epileptic drugs (see Krzemiński et al. (2020) and Routley et al. (2020) for more details about this
196 dataset). Table 1 summarizes the clinical characteristics of the individuals with epilepsy. This study
197 was approved by the South East Wales NHS ethics committee, Cardiff and Vale Research and
198 Development committees, and Cardiff University School of Psychology Research Ethics Committee.
199 Written informed consent was obtained from all participants.

200
201

202 **2.2. MEG acquisition and pre-processing**

203
204

204 MEG data were acquired using a 275-channel CTF radial gradiometer system (CTF System, Canada)
205 at a sampling rate of 600 Hz. We obtained approximately 5 minutes of MEG recordings per individual.
206 The participants were instructed to sit steadily in the MEG chair with their eyes focused on a red dot
207 on a grey background. Each individual also underwent a whole-brain T1-weighted MRI acquired using
208 a General Electric HDx 3T MRI scanner and an 8-channel receiver head coil (GE Healthcare,
209 Waukesha, WI) with an axial 3D fast spoiled gradient recalled sequence (echo time 3 ms; repetition
210 time 8 ms; inversion time 450 ms; flip angle 20°; acquisition matrix 256×192×172; voxel size 1×1×1
211 mm).

212
213

213 To assess the presence of artefacts and interictal spike wave discharges, the MEG data was divided
214 into 2 s segments and each segment was visually inspected. Artefact-free segments were identified
215 and re-concatenated for each individual. We thus obtained concatenated recordings with a variable
216 length ranging from 204 s to 300 s, and to avoid the potential impact of different recording lengths on
217 our analysis, we only considered the first 200 s of each recording for every individual. The pre-
218 processed data were then filtered in the alpha band (8-13 Hz) and down-sampled to 250 Hz. We
219 focused on the alpha band because it has been shown to be the most informative for differentiating
220 people with epilepsy from healthy controls (Schmidt et al., 2014, 2016).

221
222

223 **2.3. Source mapping from MEG**

224
225

225 To infer functional networks from the MEG data, we first mapped the data from the sensor space to
226 the source space. The MEG sensors were co-registered with the structural MRI using the locations of
227 the fiducial coils in the CTF software (MRIViewer and MRICConverter), and we obtained a volume
228 conduction model from the MRI scan using a semi-realistic model (Nolte, 2003). To reconstruct the
229 source signals, we used a linear constrained minimum variance (LCMV) beamformer on a 6-mm
230 template with a local-spheres forward model in Fieldtrip (Oostenveld et al., 2011;
231 <http://www.ru.nl/neuroimaging/fieldtrip>). We mapped the source signals into the 90 brain regions of
232 the Automated Anatomical Label (AAL) atlas (Hipp et al., 2012). For more details about these
233 methods see our previous studies (Krzemiński et al., 2020, Routley et al., 2020).

234
235

236 **2.4. Functional networks**

237

238 We divided the 200-s-long source reconstructed MEG recordings into 10, non-overlapping, 20 s
239 segments. The choice of segment length was motivated by previous studies that aimed to distinguish
240 people with epilepsy from controls using resting-state scalp EEG (Schmidt et al., 2014, 2016). For
241 each segment, we computed a functional network using the amplitude envelope correlation (AEC)
242 with orthogonalized signals (Hipp et al., 2012) (see Supplementary Material S1 for more details). We
243 selected this method because it has been shown to be a reliable measure of functional connectivity
244 (Colclough et al., 2016). To remove spurious connections, we generated 99 surrogates from the
245 original MEG signals using the iterative amplitude-adjusted Fourier transform (IAAFT) with 10
246 iterations (Schreiber and Schmitz, 1996, 2000) (surrogates are randomized time series comparable to
247 the original time series). We excluded connections if their weights did not exceed the 95%
248 significance level compared to the same connection weights as computed from the surrogates
249 (Schmidt et al., 2014, 2016, Lopes et al., 2019). Using this method, we obtained 10 functional
250 networks per individual.

251 252 253 **2.5. Mathematical model**

254
255 To study the inherent propensity of a MEG functional network to generate seizures, we placed a
256 canonical mathematical model of ictogenicity at each network node, i.e. at each of the 90 brain
257 regions represented in the functional network (Lopes et al., 2017, 2018, 2019, 2020). The activity of a
258 network node was described by a phase oscillator, which could transit between two states: a 'resting
259 state' at which the oscillator fluctuated close to a fixed stable phase and a 'seizure state' represented
260 by a rotating phase (see Supplementary Material S2 for more details about the model). This canonical
261 model has been shown to approximate the interaction between neural masses (Lopes et al., 2017).

262 263 264 **2.6. Brain network ictogenicity**

265
266 The mathematical model allowed us to generate synthetic brain activity which fluctuated between the
267 resting and the seizure states. To quantify this activity, we used the BNI (Chowdhury et al., 2014;
268 Petkov et al., 2014; Lopes et al., 2017, 2018, 2019, 2020), which is the average fraction of time that
269 the network spent in the seizure state (see Supplementary Material S3 for more details). We interpret
270 higher values of BNI as representing a higher inherent propensity of the brain to generate seizure
271 activity. Thus, although we use resting-state MEG data to infer the functional networks, we assume
272 that the underlying brain states may differ in their inherent propensity to generate seizures and this
273 may be captured by our computational framework. We expect that functional networks from JME
274 individuals should be characterized by higher values of BNI than those from healthy individuals.

275
276 The simulated synthetic activity depends on a model parameter, the global scaling coupling K (see
277 Supplementary Material S2). Higher K values imply stronger neuronal interactions between
278 connected nodes, which in turn leads to higher BNI values. Hence, for a fair comparison of BNI
279 between different functional networks, K must be the same in all simulations. To avoid an arbitrary
280 choice of K , we considered a redefinition of BNI (Lopes et al., 2018). This redefinition consists in
281 computing BNI for a sufficiently large interval of K values in order to capture the full variation of BNI
282 from 0 to 1. Then we calculated $\langle BNI \rangle$ as the integral of the BNI in this interval (see Supplementary
283 Material S3). For a meaningful comparison between different functional networks, we used the same
284 interval of K for all simulations. This procedure has been shown to be robust (Lopes et al., 2018).
285 Analogously to the BNI, a higher $\langle BNI \rangle$ value corresponds to a higher propensity of a network to
286 generate seizures. Figure 1 summarizes the key steps of our method.

287 288 289 **2.7. Statistical methods**

290
291 We computed 10 functional networks per individual and therefore we obtained 10 $\langle BNI \rangle$ values per
292 individual. We then calculated $\langle \langle BNI \rangle \rangle$, the average of the 10 $\langle BNI \rangle$ values. Finally, we used the Mann-
293 Whitney U test to assess whether the median of $\langle \langle BNI \rangle \rangle$ was higher in people with epilepsy than in the
294 healthy controls.

295 296 297 **3. Results**

298
299
300
301
302
303
304
305
306
307
308
309
310
311
312
313
314
315
316
317
318
319
320
321
322
323
324
325
326
327
328
329
330
331
332
333
334
335
336
337
338
339
340
341
342
343
344
345
346
347
348
349
350
351
352
353
354
355
356
357

We considered resting-state MEG recordings from 26 people with JME and 26 healthy controls. To test whether BNI was larger in individuals with JME than in healthy controls, we first built functional networks from MEG source reconstructed data, then we placed a mathematical model of ictogenicity into the network nodes and measured the networks' propensity to generate seizures *in silico*. Figure 2(a) shows the BNI for all individuals. Overall, individuals with JME had larger BNI values than healthy controls ($p = 0.0039$, Mann-Whitney U test). This finding confirms our hypothesis that resting-state functional networks from people with epilepsy have a higher propensity to generate seizures than those from healthy controls. Note also that for each individual, we observed that BNI had a small variance (i.e. the intraindividual BNI variability is smaller than the interindividual BNI variability), implying that BNI was consistent across the 10 different MEG resting-state functional networks of each individual. We then tested whether BNI could be used for individual classification as to whether individuals had epilepsy. Figure 2(b) shows the receiver operating characteristic (ROC) curve. The area under the curve (AUC) was 0.72, the sensitivity was 0.77, and the specificity was 0.58. The BNI 's classification accuracy was 73%.

The results in Fig. 2 may be confounded by a number of factors. Namely, epilepsy duration and seizure frequency may have an impact on the BNI values. Figure S1 shows the BNI versus these clinical characteristics in the JME group. From visual inspection, the figure suggests that while individuals with short epilepsy duration or low seizure frequency may exhibit both low and high BNI values, individuals with relatively longer epilepsy duration (larger than 20 years) and higher seizure frequency (higher than 200 seizures per year) present high BNI values.

4. Discussion

To date, the BNI framework has proved to be valuable for the diagnosis of IGE using scalp EEG (Schmidt et al., 2014, 2016; Petkov et al., 2014), assessment of epilepsy surgery using intracranial EEG (Goodfellow et al., 2016; Lopes et al., 2017, 2018, 2020; Laiou et al., 2019), and epilepsy classification using scalp EEG (Lopes et al., 2019). Here we aimed to test whether the concept of BNI could differentiate people with JME from age and gender matched healthy controls using resting-state MEG data. We found that the BNI is on average higher in the JME group than in the control group. We further found that, as a classifier, the BNI yields a sensitivity of 0.77, a specificity of 0.58, and an AUC of 0.72, which is similar to previous findings in IGE using scalp EEG (Schmidt et al., 2016). This result suggests that MEG and scalp EEG may yield similar diagnostic power despite MEG being considered superior to EEG in recording reliable brain signals (Supek and Aine, 2016). In other words, this suggests that the key functional network properties that characterize the underlying brain ictogenicity may be similarly captured by MEG and scalp EEG.

Resting-state MEG functional networks have been previously shown to be altered in people with epilepsy relative to healthy controls (van Dellen et al., 2012; Niso et al., 2015; Hsiao et al., 2015; Wu et al., 2017; Routley et al., 2020). For example, Niso et al. (2015) used 15 graph-theoretic measures to quantify resting-state MEG functional networks from people with frontal focal epilepsy, generalized epilepsy and healthy individuals. They found that functional networks from generalized epilepsy had greater efficiency and lower eccentricity than those from controls, whereas functional networks from frontal focal epilepsy exhibited only reduced eccentricity over fronto-temporal and central sensors relative to networks from controls. Furthermore, machine learning has been used to also differentiate people with epilepsy from controls (Soriano et al., 2017). Our study distinguishes from these studies by not only searching for differences between functional networks in health and disease, but instead test a specific mechanistic hypothesis that justifies the difference. Thus, our approach is more readily interpretable and may offer insight into why altered functional networks underlie epilepsy.

We acknowledge that our study has some limitations. First, in order to truly test how MEG-based predictions compare to scalp EEG-based predictions, we would need both MEG and EEG data collected from the same participants. Future work should assess whether predictions based on both data modalities would deliver equivalent individual classification. Second, people with JME were taking anti-epileptic medication, which may have potentially reduced the BNI in some JME individuals, making them indistinguishable from healthy individuals. Future studies should consider newly diagnosed drug-naïve individuals. This may be particularly important to also control for the effect of epilepsy duration and seizure frequency on BNI. Our results suggest that individuals with longer

358 epilepsy duration and higher seizure frequency were more likely to be characterized by high BNI. On
359 one hand this is an expected observation, i.e. BNI should be higher for individuals more prone to
360 seizures and also those for which a longer disease may have had an impact on resting-state
361 functional connectivity. On the other hand, these were individuals for which diagnosis could be less
362 challenging. Third, we focused our analysis on differentiation of people with JME from healthy
363 controls. We therefore cannot exclude the possibility that our findings are specific to JME. More
364 comprehensive datasets will be needed to explore whether our findings generalize to other types of
365 epilepsy.

366

367

368 **5. Conclusions**

369

370 Our results demonstrate that the BNI framework generalizes from scalp EEG to MEG. We showed
371 that resting-state MEG from people with JME is characterized by higher BNI than that from healthy
372 controls. The achieved classification accuracy is similar to previously obtained from scalp EEG,
373 suggesting that the two data modalities may capture similar underlying ictogenic features.

374

375

376 **6. References**

377

378 Abela, E., Pawley, A. D., Tangwiriyasakul, C., Yaakub, S. N., Chowdhury, F. A., Elwes, R. D., ... &
379 Richardson, M. P. (2019). Slower alpha rhythm associates with poorer seizure control in epilepsy.
380 *Annals of clinical and translational neurology*, 6(2), 333-343. doi: 10.1002/acn3.710

381

382 Benbadis, S. (2009). The differential diagnosis of epilepsy: a critical review. *Epilepsy & Behavior*,
383 15(1), 15-21. doi: 10.1016/j.yebeh.2009.02.024

384

385 Benbadis, S. R., Beniczky, S., Bertram, E., MacIver, S., & Moshé, S. L. (2020). The role of EEG in
386 patients with suspected epilepsy. *Epileptic Disorders*, 22(2), 143-155. doi: 10.1684/epd.2020.1151

387

388 Chowdhury, F. A., Woldman, W., FitzGerald, T. H., Elwes, R. D., Nashef, L., Terry, J. R., &
389 Richardson, M. P. (2014). Revealing a brain network endophenotype in families with idiopathic
390 generalised epilepsy. *PloS one*, 9(10), e110136. doi: 10.1371/journal.pone.0110136

391

392 Colclough, G. L., Woolrich, M. W., Tewarie, P. K., Brookes, M. J., Quinn, A. J., & Smith, S. M. (2016).
393 How reliable are MEG resting-state connectivity metrics?. *Neuroimage*, 138, 284-293. doi:
394 10.1016/j.neuroimage.2016.05.070

395

396 Coito, A., Genetti, M., Pittau, F., Iannotti, G. R., Thomschewski, A., Höller, Y., ... & Plomp, G. (2016).
397 Altered directed functional connectivity in temporal lobe epilepsy in the absence of interictal spikes: a
398 high density EEG study. *Epilepsia*, 57(3), 402-411. doi: 10.1111/epi.13308

399

400 van Dellen, E., Douw, L., Hillebrand, A., Ris-Hilgersom, I. H., Schoonheim, M. M., Baayen, J. C., ... &
401 Stam, C. J. (2012). MEG network differences between low-and high-grade glioma related to epilepsy
402 and cognition. *PloS one*, 7(11). doi: 10.1371/journal.pone.0050122

403

404 Hipp, J. F., Hawellek, D. J., Corbetta, M., Siegel, M., & Engel, A. K. (2012). Large-scale cortical
405 correlation structure of spontaneous oscillatory activity. *Nature neuroscience*, 15(6), 884. doi:
406 10.1038/nn.3101

407

408 Horstmann, M. T., Bialonski, S., Noennig, N., Mai, H., Prusseit, J., Wellmer, J., ... & Lehnertz, K.
409 (2010). State dependent properties of epileptic brain networks: Comparative graph-theoretical
410 analyses of simultaneously recorded EEG and MEG. *Clinical Neurophysiology*, 121(2), 172-185. doi:
411 10.1016/j.clinph.2009.10.013

412

413 Hsiao, F. J., Yu, H. Y., Chen, W. T., Kwan, S. Y., Chen, C., Yen, D. J., ... & Lin, Y. Y. (2015).
414 Increased intrinsic connectivity of the default mode network in temporal lobe epilepsy: evidence from
415 resting-state MEG recordings. *PLoS One*, 10(6). doi: 10.1371/journal.pone.0128787

416

- 417 Krzemiński, D., Masuda, N., Hamandi, K., Singh, K. D., Routley, B., & Zhang, J. (2020). Energy
418 landscape of resting magnetoencephalography reveals fronto-parietal network impairments in
419 epilepsy. *Network Neuroscience*, 1-23. doi: 10.1162/netn_a_00125
420
- 421 Laiou, P., Avramidis, E., Lopes, M. A., Abela, E., Müller, M., Akman, O. E., ... & Goodfellow, M.
422 (2019). Quantification and selection of ictogenic zones in epilepsy surgery. *Frontiers in neurology*, 10,
423 1045. doi: 10.3389/fneur.2019.01045
424
- 425 Larsson, P. G., & Kostov, H. (2005). Lower frequency variability in the alpha activity in EEG among
426 patients with epilepsy. *Clinical Neurophysiology*, 116(11), 2701-2706. doi:
427 10.1016/j.clinph.2005.07.019
428
- 429 Lopes, M. A., Richardson, M. P., Abela, E., Rummel, C., Schindler, K., Goodfellow, M., & Terry, J. R.
430 (2017). An optimal strategy for epilepsy surgery: Disruption of the rich-club?. *PLoS computational*
431 *biology*, 13(8), e1005637. doi: 10.1371/journal.pcbi.1005637
432
- 433 Lopes, M. A., Richardson, M. P., Abela, E., Rummel, C., Schindler, K., Goodfellow, M., & Terry, J. R.
434 (2018). Elevated ictal brain network ictogenicity enables prediction of optimal seizure control.
435 *Frontiers in neurology*, 9, 98. doi: 10.3389/fneur.2018.00098
436
- 437 Lopes, M. A., Perani, S., Yaakub, S. N., Richardson, M. P., Goodfellow, M., & Terry, J. R. (2019).
438 Revealing epilepsy type using a computational analysis of interictal EEG. *Scientific reports*, 9(1), 1-10.
439 doi: 10.1038/s41598-019-46633-7
440
- 441 Lopes, M. A., Junges, L., Tait, L., Terry, J. R., Abela, E., Richardson, M. P., & Goodfellow, M. (2020).
442 Computational modelling in source space from scalp EEG to inform presurgical evaluation of epilepsy.
443 *Clinical Neurophysiology*, 131(1), 225-234. doi: 10.1016/j.clinph.2019.10.027
444
- 445 Niso, G., Carrasco, S., Gudín, M., Maestú, F., del-Pozo, F., & Pereda, E. (2015). What graph theory
446 actually tells us about resting state interictal MEG epileptic activity. *Neuroimage: clinical*, 8, 503-515.
447 doi: 10.1016/j.nicl.2015.05.008
448
- 449 Nolte, G. (2003). The magnetic lead field theorem in the quasi-static approximation and its use for
450 magnetoencephalography forward calculation in realistic volume conductors. *Physics in Medicine &*
451 *Biology*, 48(22), 3637. doi: 10.1088/0031-9155/48/22/002
452
- 453 Oostenveld, R., Fries, P., Maris, E., & Schoffelen, J. M. (2011). FieldTrip: open source software for
454 advanced analysis of MEG, EEG, and invasive electrophysiological data. *Computational intelligence*
455 *and neuroscience*, 2011, 1. doi: 10.1155/2011/156869
456
- 457 Petkov, G., Goodfellow, M., Richardson, M. P., & Terry, J. R. (2014). A critical role for network
458 structure in seizure onset: a computational modeling approach. *Frontiers in neurology*, 5, 261. doi:
459 10.3389/fneur.2014.00261
460
- 461 Pillai, J., & Sperling, M. R. (2006). Interictal EEG and the diagnosis of epilepsy. *Epilepsia*, 47, 14-22.
462 doi: 10.1111/j.1528-1167.2006.00654.x
463
- 464 Quraan, M. A., McCormick, C., Cohn, M., Valiante, T. A., & McAndrews, M. P. (2013). Altered resting
465 state brain dynamics in temporal lobe epilepsy can be observed in spectral power, functional
466 connectivity and graph theory metrics. *PloS one*, 8(7). doi: 10.1371/journal.pone.0068609
467
- 468 Routley, B., Shaw, A., Muthukumaraswamy, S. D., Singh, K. D., & Hamandi, K. (2020). Juvenile
469 myoclonic epilepsy shows increased posterior theta, and reduced sensorimotor beta resting
470 connectivity. *Epilepsy Research*, 106324. doi: 10.1016/j.eplepsyres.2020.106324
471
- 472 Schmidt H., Petkov G., Richardson M.P., Terry J.R. (2014) Dynamics on networks: the role of local
473 dynamics and global networks on the emergence of hypersynchronous neural activity. *PLoS Comput*
474 *Biol*, 10:e1003947. doi: 10.1371/journal.pcbi.1003947
475

476 Schmidt H., Woldman W., Goodfellow M., Chowdhury F.A., Koutroumanidis M., Jewell S., et al.
 477 (2016) A computational biomarker of idiopathic generalized epilepsy from resting state EEG.
 478 *Epilepsia*, 57:e200–4. doi: 10.1111/epi.13481
 479
 480 Schreiber, T., & Schmitz, A. (1996). Improved surrogate data for nonlinearity tests. *Physical review*
 481 *letters*, 77(4), 635. doi: 10.1103/PhysRevLett.77.635
 482
 483 Schreiber, T., & Schmitz, A. (2000). Surrogate time series. *Physica D: Nonlinear Phenomena*, 142(3-
 484 4), 346-382. doi: 10.1016/S0167-2789(00)00043-9
 485
 486 Smith, S. J. M. (2005). EEG in the diagnosis, classification, and management of patients with
 487 epilepsy. *Journal of Neurology, Neurosurgery & Psychiatry*, 76(suppl 2), ii2-ii7. doi:
 488 10.1136/jnnp.2005.069245
 489
 490 Soriano, M. C., Niso, G., Clements, J., Ortín, S., Carrasco, S., Gudín, M., ... & Pereda, E. (2017).
 491 Automated detection of epileptic biomarkers in resting-state interictal MEG data. *Frontiers in*
 492 *neuroinformatics*, 11, 43. doi: 10.3389/fninf.2017.00043
 493
 494 Supek, S., & Aine, C. J. (2016). *Magnetoencephalography*. Springer-Verlag Berlin An. doi:
 495 10.1007/978-3-642-33045-2
 496
 497 van Diessen, E., Otte, W. M., Braun, K. P., Stam, C. J., & Jansen, F. E. (2013). Improved diagnosis in
 498 children with partial epilepsy using a multivariable prediction model based on EEG network
 499 characteristics. *PLoS one*, 8(4). doi: 10.1371/journal.pone.0059764
 500
 501 van Diessen, E., Otte, W. M., Stam, C. J., Braun, K. P., & Jansen, F. E. (2016).
 502 Electroencephalography based functional networks in newly diagnosed childhood epilepsies. *Clinical*
 503 *Neurophysiology*, 127(6), 2325-2332. doi: 10.1016/j.clinph.2016.03.015
 504
 505 Verhoeven, T., Coito, A., Plomp, G., Thomschewski, A., Pittau, F., Trinka, E., ... & Dambre, J. (2018).
 506 Automated diagnosis of temporal lobe epilepsy in the absence of interictal spikes. *NeuroImage:*
 507 *Clinical*, 17, 10-15. doi: 10.1016/j.nicl.2017.09.021
 508
 509 WHO (2019) <https://www.who.int/news-room/fact-sheets/detail/epilepsy>
 510
 511 Wu, C., Xiang, J., Jiang, W., Huang, S., Gao, Y., Tang, L., ... & Wang, X. (2017). Altered effective
 512 connectivity network in childhood absence epilepsy: a multi-frequency MEG study. *Brain topography*,
 513 30(5), 673-684. doi: 10.1007/s10548-017-0555-1
 514
 515
 516
 517
 518
 519
 520
 521

ID	Age	Gender	Epilepsy duration	Seizure frequency		
				MJ	ABS	GTCS
JME1	17.8	f	2.8	12	365	3
JME2	31.3	f	18.3	12	12	1
JME3	27	f	19.0	104	0	1
JME4	20.1	f	3.1	0	0	4
JME5	20.7	f	3.7	4	4	4
JME6	20.4	f	5.4	12	0	104
JME7	19.2	f	4.2	12	12	12
JME8	20.9	f	12.9	104	36	4
JME9	35.3	f	23.3	2920	0	1
JME10	30.2	m	16.2	52	52	4
JME11	23.7	m	8.7	365	2	2

JME12	38.8	f	21.8	365	365	104
JME13	22.2	m	4.2	104	0	52
JME14	33.1	f	21.1	12	1	12
JME15	29.7	m	14.7	12	0	0
JME16	25.7	f	10.7	6	12	1
JME17	36	f	27.0	0	365	12
JME18	38.6	f	28.6	2	0	1
JME19	44.3	m	29.3	365	365	2
JME20	47.7	f	40.7	52	52	1
JME21	26.8	m	8.8	1	0	0
JME22	22.3	f	10.3	6	0	1
JME23	38.7	f	24.7	0	0	1
JME24	18.9	f	3.9	0	0	1
JME25	31.1	f	18.1	1	0	0.2
JME26	22.7	m	10.7	1	1	0.2

522 Table 1: Clinical characteristics of the individuals with JME. Age and epilepsy duration are in years, m
 523 = male, f = female, seizure frequency is in number of seizures per year and is divided in three types of
 524 epileptiform activity: MJ = myoclonic jerks, ABS = absence seizures, and GTCS = generalized tonic-
 525 clonic seizures. Seizure frequency was based on self-reporting at the time of scan and extrapolated to
 526 a number of seizures per year.

527

528

529 Figure Legends

530

531 Figure 1

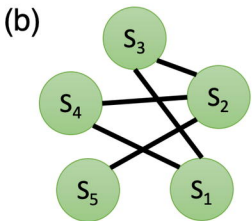
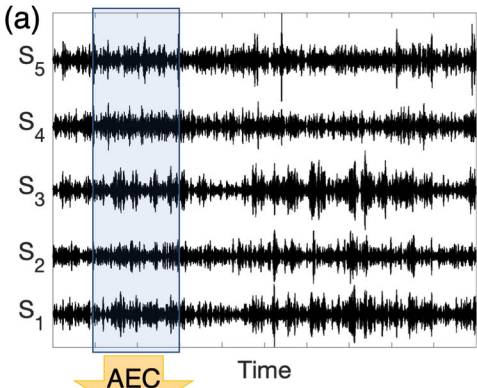
532 Scheme of the data analysis procedure to compute \widehat{BNI} . (a) We select a MEG source reconstructed
 533 data segment and by measuring the AEC we obtain (b) a functional network. To assess the
 534 propensity of the network to generate seizures, we then use (c) the theta model to simulate (d)
 535 synthetic brain activity. We then calculate (e) the BNI, i.e. the average fraction of time that network
 536 nodes spend in seizure-like activity. To avoid an arbitrary choice of K , we compute (f) BNI as a
 537 function of K . (g) \widehat{BNI} is then the integral of BNI in the interval $[K_1, K_2]$, i.e. the area under the BNI
 538 curve.

539

540

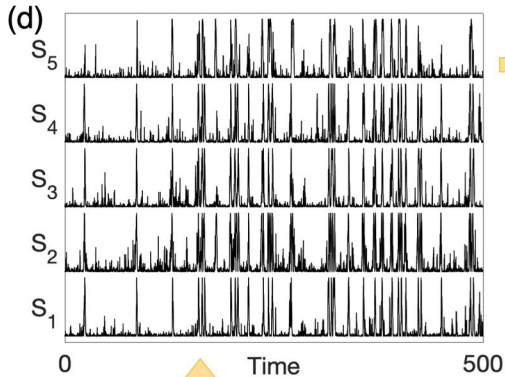
541 Figure 2

542 Brain network ictogenicity (\widehat{BNI}) in healthy individuals and people with JME. Each marker in panel (a)
 543 represents the average \widehat{BNI} (i.e. $\langle \widehat{BNI} \rangle$) of a single individual and the error bars their standard error
 544 computed from 10 MEG resting-state functional networks. Blue markers correspond to healthy
 545 individuals, whereas red markers correspond to individuals with epilepsy. The epilepsy group has a
 546 larger $\langle \widehat{BNI} \rangle$ than the healthy group ($p = 0.0039$, Mann-Whitney U test). Panel (b) shows the receiver
 547 operating characteristic (ROC) curve for one group versus the other using the $\langle \widehat{BNI} \rangle$ as a classifier.
 548 The area under the curve (AUC) is 0.72 and the circle identifies the optimal operating point of the
 549 ROC curve, for which the sensitivity is 0.77, and the specificity is 0.58.



(c)

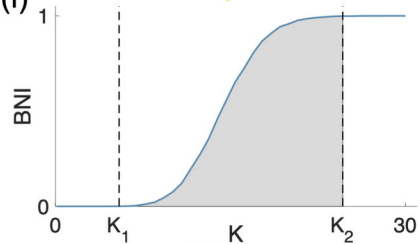
Place theta model onto the nodes of the network and simulate transitions between resting and seizure-like states.



(e)

Compute BNI, the average fraction of time the network spends in the seizure-like state.

(f)



(g)

\widehat{BNI} = area under the BNI curve

